Full Length Research Paper

Efficient calculation of operating security regions in power systems

E. A. Al-Ammar[1,2]* and M. A. El-Kady[1,2]

[1]Center of Excellence in Information Assurance (CoEIA), King Saud University, Riyadh, Saudi Arabia.
[2]Department of Electrical Engineering, College of Engineering, King Saud University, Riyadh 11421, Saudi Arabia.

Power system operators are often faced with the challenge of identifying the dynamic operating security modes during the on-line operation of the power system, which requires fast, accurate and reliable evaluation techniques. The system security constraints are in fact boundaries that surround all possible operating modes (scenarios) of the power system. In other words, these boundaries form the feasible operating domain - in the parameter space spanned by various operating variables - within which the system can safely be operated. For a given operating scenario, the associated security level is measured by the "distance" (for example, the Euclidean norm) of the operating point from the security region boundary. This paper presents a novel methodology and computerized scheme, which are capable of identifying dynamic operating security modes during the on-line operation of electric power systems. The methodology adopted in this paper includes the development of advanced, highly efficient computerized algorithms for fast identification of dynamic operating security modes of power systems. One of the salient outcomes of this paper is the development of a novel framework for identification and representation of operating security regions in power systems as well as evaluation of security levels associated with different operating scenarios. While the concepts and principles presented are general, the work of this paper is confined to the interpretation of the security boundary in terms of system stability criteria. In addition, the framework presented is applicable quite as well to other criteria that may be considered.

Key words: Power system operation, security regions, system stability, operating constraints.

INTRODUCTION

The importance of efficient and secure operation of the power grid has always been acknowledged by the electric power utilities. In this regard, power system operation aims, in principle, at maintaining reliable and secure supply of electricity while minimizing the total cost of operation. In theory, there are two main objectives that could be considered, namely the maximization of system security and the minimization of total operating cost of supplying energy (Tomsovic et al., 1993; El-Kady, 1986; Albert and Hyde, 1974; Benguo et al., 2006). In practice, however, the security requirements are included as constraints rather than formulating the problem as security maximization

mandate (El-Kady et al., 1986a, b, c; Allen and Bruce, 1984; Annakkage and Jayasekara, 2007; Aven, 2007; Popovic et al., 2001). The system security constraints are in fact boundaries that surround all possible operating modes (scenarios) of the power system. In other words, these boundaries form the feasible operating domain - in the parameter space spanned by various operating variables - within which the system can safely be operated. For a given operating scenario, the associated security level is measured by the "distance" (for example, the Euclidean norm) of the operating point from the security region boundary (Zeng et al., 2006; Aghaei et al., 2009; El-Kady and Ganton, 1989; Srivani and Swarup, 2008; Athay et al., 1979; El-Kady et al., 1986a, b, c).

Security constraints could either be "static" or "dynamic". The term "static security" means that all constraints reflect steady-state quantities such as steady-

---
*Corresponding author. E-mail: essam@ksu.edu.sa. Tel: +96614670593. Fax: +96614676757.
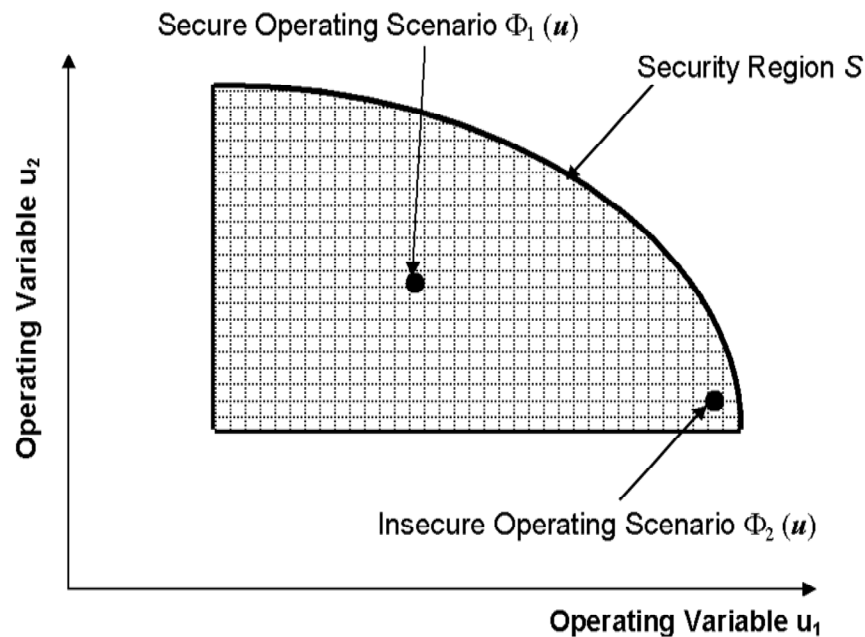
Figure 1. Illustration of operating security region.

state bus voltage violations and steady-state transmission line overloading. In conventional approaches, the dynamic security constraints are either neglected or checked subsequently and independent of the operating cost minimization scheme. In real power system operations, however, any re-distribution of generator powers to minimize fuel costs (economic dispatch) would also influence the system dynamic behavior (stability) when a contingency occurs (for example, a fault which is cleared by a transmission line outage). Modeling complexity as well as the multi-discipline nature of the research required have traditionally prevented the inclusion of the dynamic system security constraints in the overall optimization procedure, which would include both static and dynamic security constraints. While the static security constraints ensure that the system integrity is maintained during the steady-state operation, the dynamic security constraints ensure that the system would maintain its dynamic robustness during contingency situations. In addition to static and dynamic security constraints, other boundaries are defined, for example, in terms of equipment physical constraints (El-Kady and Ammar, 2009; Al-Ammar and El-Kady, 2009).

This paper reports on the results of a recently completed research and development project, which included the development of innovative computerized schemes, which are capable of identifying dynamic operating security modes during the on-line operation of electric power systems. These identified secure operating modes are extremely valuable for power system operators who are responsible for maintaining the security and reliability of the power system on a continuous basis. The methodology adopted in this paper includes the development of advanced, highly efficient computerized algorithms for fast identification of dynamic operating security modes of power systems.

One of the salient outcomes of this paper is the development of a novel framework for identification and representation of operating security regions in power systems as well as evaluation of security levels associated with different operating scenarios. While the concepts and principles presented are general, the work of this paper is confined to the interpretation of the security boundary in terms of system stability criteria. Of course, the framework presented is applicable quite as well to other criteria that may be considered.

Background and problem formulation

The schematic representation of Figure 1 illustrates the concept of operating security region, where the level of security associated with different operating scenarios is measured in terms of how far the operating point is from the security boundaries.

In formulating the problem on hand, we denote by $\Re$ the field of real numbers. The vector space over $\Re$, of n-tuples $(z_1, z_2, ..., z_n)$, $z_i \in \Re$ is denoted by $\Re^n$. We classify the problem variables into two groups, namely the state

variables $x_i \in \Re^n$, which are grouped into the column vector x, and the control variables $u_k \in \Re^m$, which are grouped into the column vector u. We note that the states x_i are those variables which are of interest to the problem but can only be observed (for example, transmission line flows), while the controls u_k are those variables which can be adjusted (manipulated) in practice (for example, plant output powers, var additions, etc.). The state and control variables are related through as set of n equality constraints $h(x, u) = 0$ representing, for example, the network flow equations. A set of potential operating scenarios $\Phi_l (u)$, l =1, 2, .., N_L is defined to represent different groupings of the control variables associated with particular operating decisions that cause the power system to reside in a particular mode of operation. In other words, $\Phi_l (u)$ defines a particular setting $\{u_k^L \in \Re^m\}$ of the system operating modes resulting from certain operator decisions.

Now the security assessment problem is formulated in terms of a *System Security Index* f(x,u) which measures the distance, in terms of a particular norm (for example, Euclidean norm), of a particular system operating mode and the so-called operating security region S. The security region S is the feasible space spanned by the problem variables within which all operating scenarios are considered secure. Therefore, the security region S is defined, in general, by a number of inequality constraints $g(x, u) \geq 0$, which may include – as special case - simple upper and lower bounds on the state and control variables $x^L \leq x \leq x^U$ & $u^L \leq u \leq u^U$. In the present work, the system security index f(x, u) will be defined as the minimum of the distance norms between a feasible operating scenario and all relevant inequality constraints. In other words   f(x, u) = Minimum {over j} of $|g_j(x, \Phi_l (u))|$, where $g_j(x, \Phi_l (u))$ is the value of the j-th inequality constraint evaluated at the operating scenario $\Phi_l (u)$. Obviously large values of f(x, u) would indicate more secure operating modes.

In order to deal with the presence of the state variables in the problem formulation in an efficient and proper mathematical manner, the concept of reduced gradients (total derivatives) could be employed.

The reduced gradients of the system security index f(x, u) with respect to the control variables u are denoted by df/du and, therefore, represent the sensitivity of the system security index f with respect to u in the sub-space spanned solely by the control variables. The reduced gradients can be calculated using the method of Lagrange multipliers, in which the partial derivatives of f(x,u) with respect to both x and u are denoted by $f_x = [\partial f / \partial x]$ and $f_u = [\partial f / \partial u]$, respectively, while the partial derivatives of the equality constraints h (x,u) with respect to both x and u are denoted by $H_x = [\partial h^T / \partial x]^T$ and $H_u = [\partial h^T / \partial u]^T$, respectively. The Lagrange multipliers are obtained by solving the set of linear equations $H_x^T \lambda = f_x$

and are then used to calculate the reduced gradients as df/du = $[f_u – H_u^T \lambda]$. It is important to note that the reduced gradients df/du represent a very powerful means for measuring the sensitivity of the system security level with respect to various operating decision variables. In other words, they provide invaluable information on how the system security is impacted by various operating decisions made by the system operators.

METHODOLOGY

In this demonstrative application scenario, a portion of an interconnected power system in North America reported in [Zeng et al., 2006] is considered, as shown in Figure 2. Two control variables representing important interface flows (I-1 and I-2) in the system will be considered in this illustrative case scenario as depicted in Figure 2. The security threshold used in this application is considered to be the theoretical transient stability limit, although in practical operating scenarios this threshold is usually specified as a percentage of the stability limit (for example 90% of the theoretical limit).

Using repetitive simulation runs for various combinations of interface flow values, the security region is drawn in the variable-space spanned by the two control variables (interface flows), as shown in Figure 3. In each simulation run, a full transient stability analysis if performed with system data altered to attain the specified values of the two control variables. The security limit values (the security region boundary) are obtained be interpolation/extrapolation over those points close to the system stability limit.

The operating security margins associated with various combinations of the control variables (interface flows in this case), which define different possible system operating scenarios, are evaluated using appropriate arithmetic norms. In the present application, the minimum per-unit distance in the Euclidean-space (of the control variables) between the operating scenario point and the closest point on the surrounding binding (active) constraints is used to indicate the operating security margin.

The following two important observations can be made from the results of Figure 3:

1. Only the binding (active) constraints are used to form the operating security region. In the present application, the binding constraints represent the system stability limits as well as the minimum load supply requirements. The non-binding (inactive) constraints (for example, the line flow limits) do not participate in forming the operating security region.

2. Two operating scenarios were considered in the demonstrative scenario of Figure 3. The first operating scenario is defined by the pair values of 775 and 900 MW of the two interface flows, respectively, while the second operating scenario is defined by the pair values of 1150 and 700 MW of the two interface flows, respectively. The evaluated operating security margins associated with the two operating scenarios are 0.92 and 0.07, respectively. The second operating scenario is therefore considered as insecure since any unforeseen deviations in the control parameters around the base operating point could lead to system instability.

RESULTS AND DISCUSSION

System model

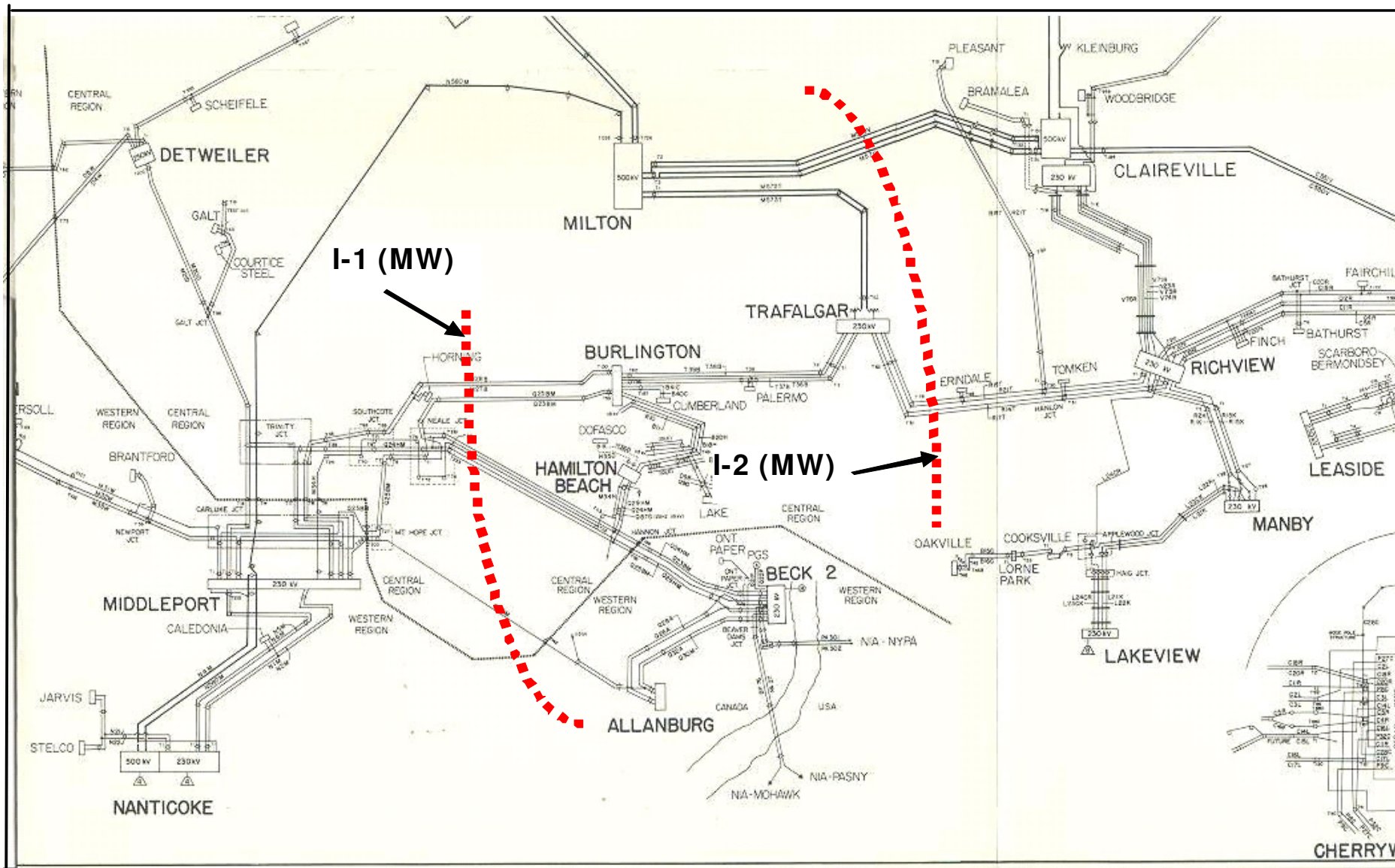In this section, applications will be presented using an

Figure 2. Illustrative security assessment study area (Zeng et al., 2006).
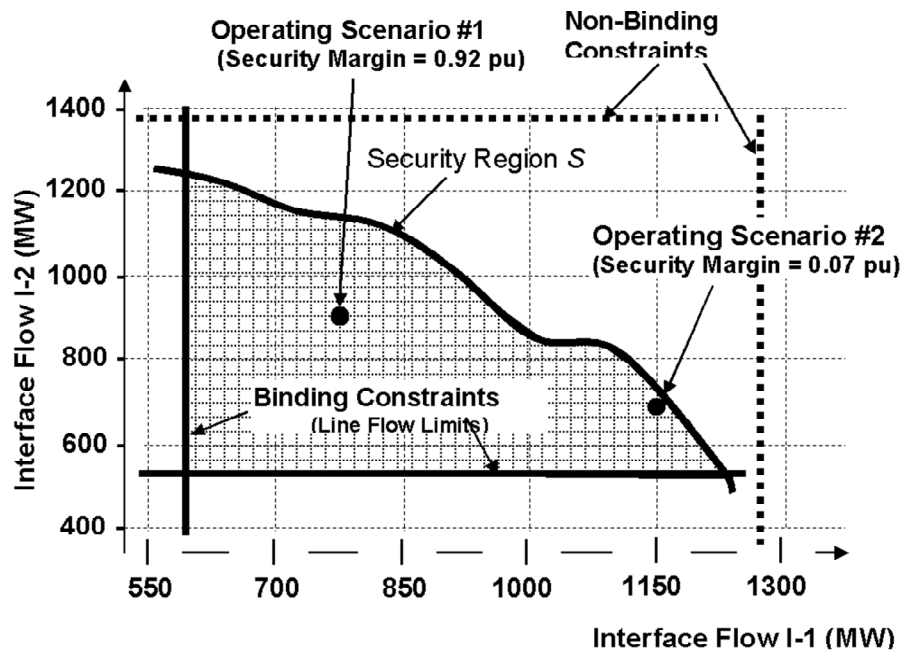
Figure 3. Operating security region for illustrative case scenario.

actual model of the Saudi electricity system. The power system used in the applications is the interconnected Saudi Electricity Company (SEC) power grid. This power system consists of two main regions, namely the SEC-C (Central Region), SEC-E (Eastern Region). The two SEC systems are interconnected through two 380 kV and one 230 kV double-circuit lines. In the original (unreduced) load-flow system model, the interconnected SEC bulk electricity system comprises 150 generator buses, 637 load buses, a total of 1168 transmission lines and transformers. In order to prepare a number of meaningful system models, which are suitable for the present security assessment studies, a reduced network model derived from the original base-case is used, which comprises 119 buses (19 generators, 100 loads), 334 lines and 122 transformers. This system model will be referred to as the 19-Generator model. The nineteen generators are distributed as 11 in the SEC-C area, 8 in the SEC-E area as shown in Figure 4.

Operating security in domain of PP8 - Qassim Powers

In this scenario, the total output powers from both the PP8 power plant and Qassim area are considered. The associated operating security margin is evaluated in the space spanned by these two output powers. A special simulation module was used to evaluate the impacts on system security as a result of variations in the output powers. Figure 5a shows the variation of the operating security margin (energy margin) with PP8 output power level. It is clear from the results of Figure 5a that the security level decreases as the output power from PP8 increases. The insecure region (zero energy margin) starts at the PP8 output level of about 14 PU. The sensitivity information of Figure 5a is also of particular interest and can be used to examine the relative system security. For example, it is noted that an increase in PP8 power level by 2.5 PU from a base operating level of 10 PU would cause the energy margin to decrease from 24 PU to about 10 PU. This represents a security deterioration of about 58% for an increase in output power by just 25%.

On the other hand, Figure 5b shows the variation of the operating security margin (energy margin) with Qassim output power level. It is clear from the results of Figure 5b that the security level decreases as the output power from Qassim increases. The insecure region (zero energy margin) starts at the Qassim output level of about 11.3 PU. Again, the sensitivity information of Figure 5b can be used to examine the relative system security. For example, an increase in Qassim power level by 4 PU from a base operating level of 4 PU would cause the energy margin to decrease from 29 PU to about 13 PU. This represents a security deterioration of about 55% for an increase in output power by 200%. Comparing this result with that of PP8, it is concluded that the relative increase in Qassim power output has a lesser impact on system security than that of the PP8. This finding is confirmed from the results of Figure 5c, which depicts the
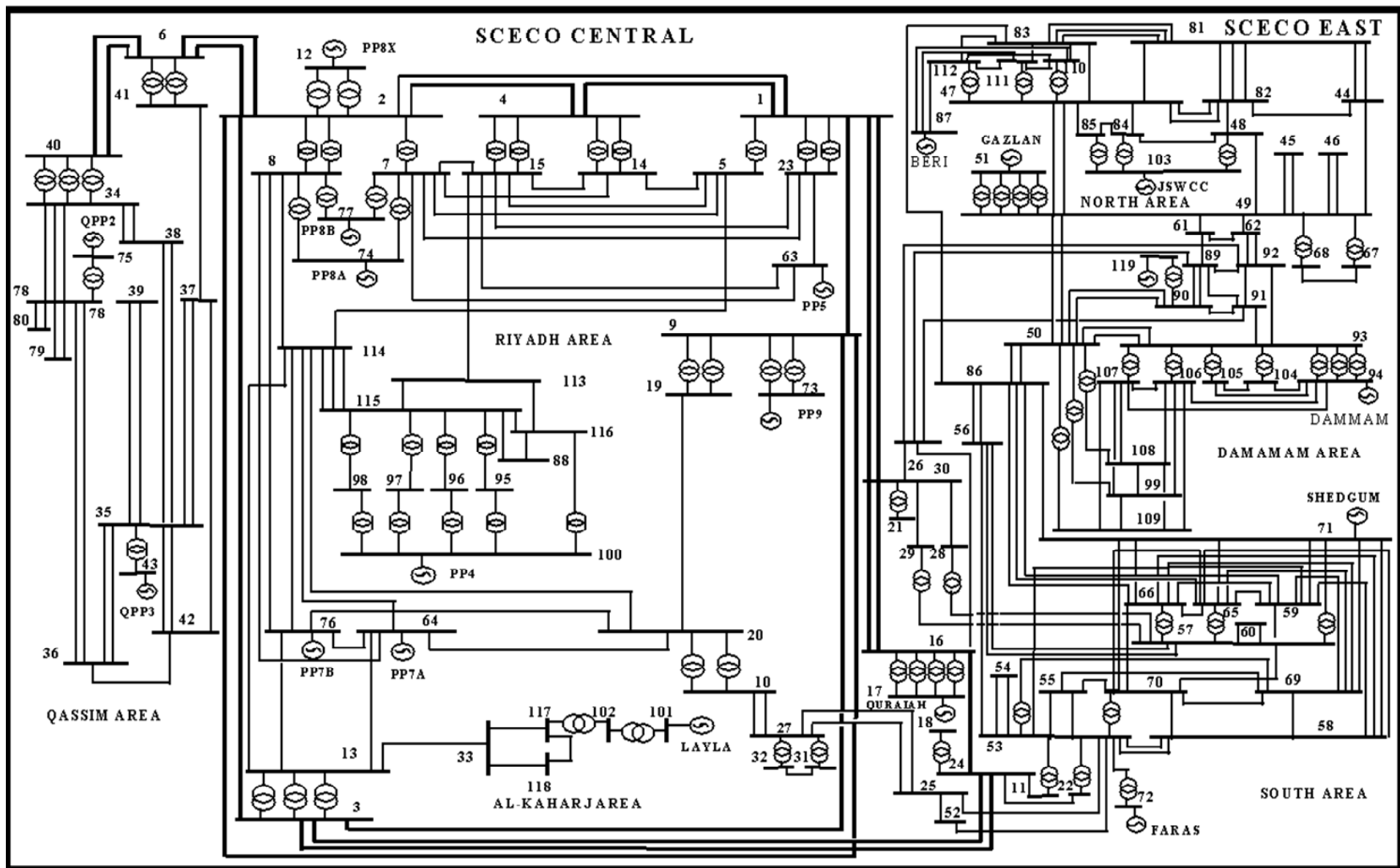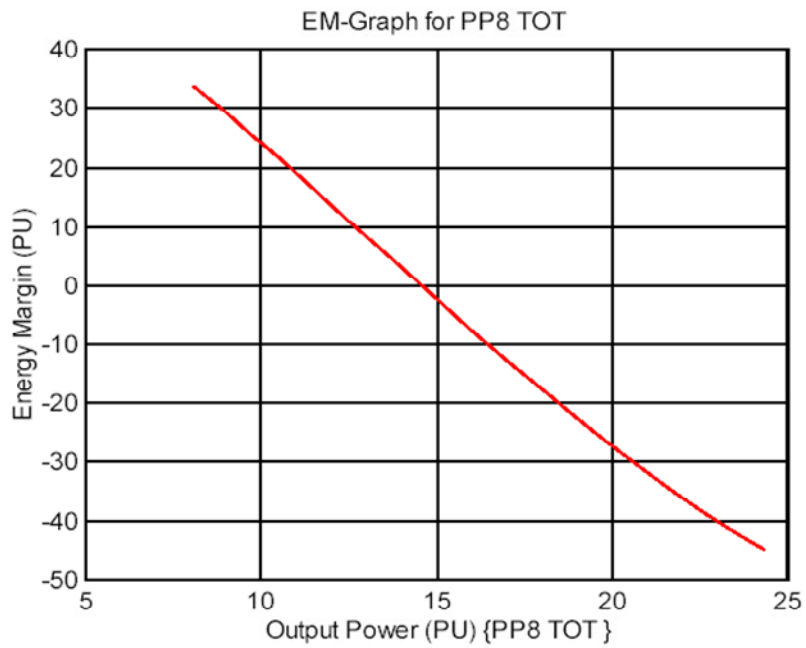
Figure 4. SEC 19-Generators System Model.

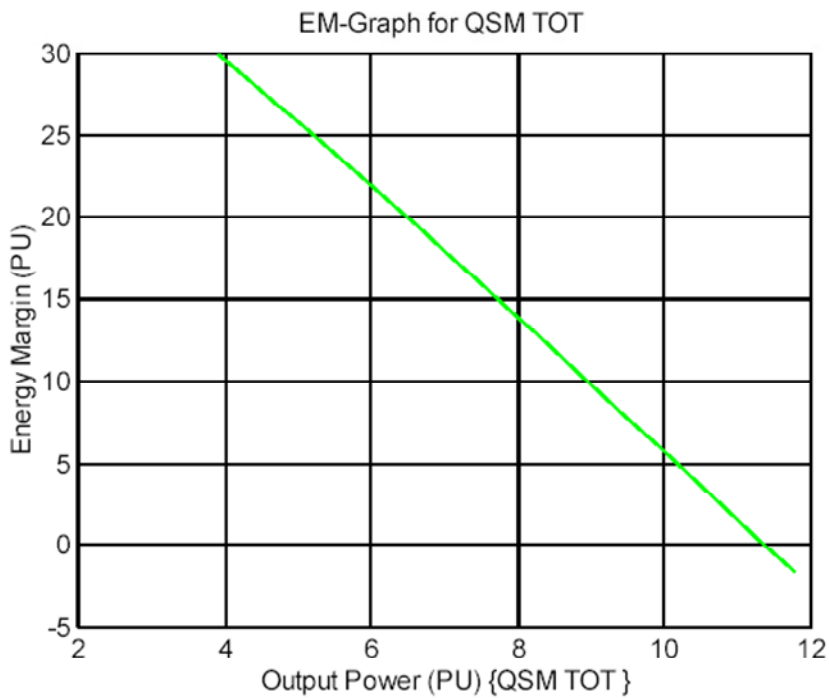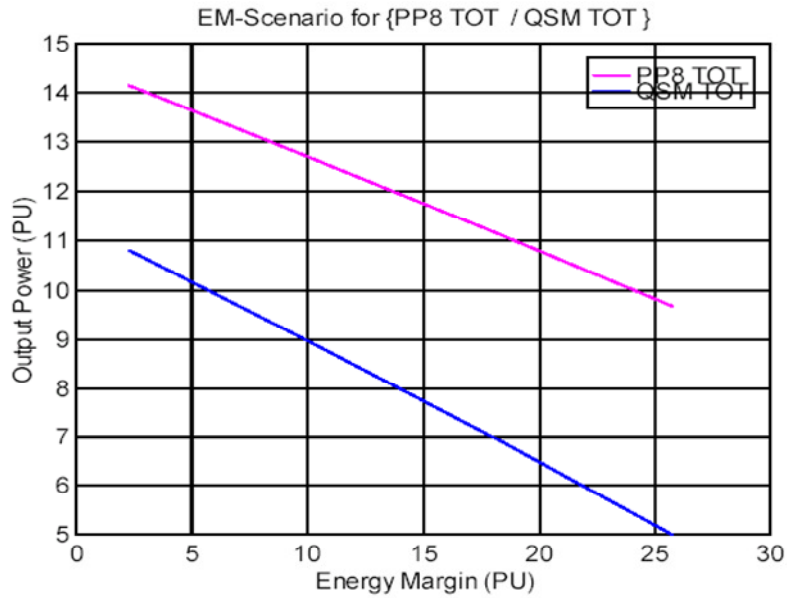**Figure 5a.** Operating security margin versus PP8 output power.

**Figure 5b.** Operating security margin versus Qassim output power.

relationship between the two output powers and the system energy margin.

Another powerful feature of the security assessment simulation is the so called "energy margin contours", which depict possible combined variations of both PP8 and Qassim output powers for a given system security

Figure 5c. Relationship between PP8 and Qassim output powers and energy margin.
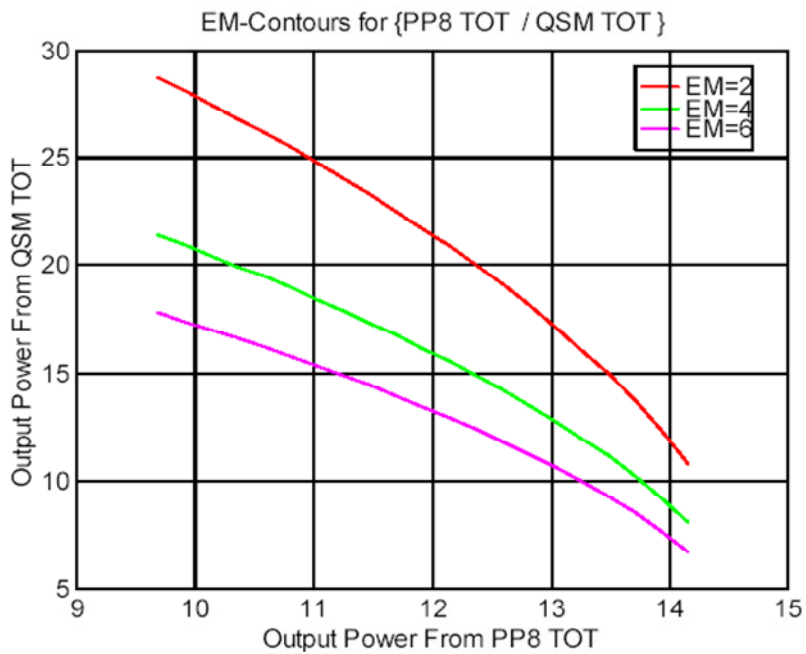
Figure 5d. Energy margin contours in the domain of PP8 and Qassim output powers.

level. Figure 5d shows three energy margin contours at 2, 4, and 6 PU values, respectively. It is important to note that, unlike the previous relationships of Figures 5a to 5c, which apply to one system operating scenario, the energy margin contours are evaluated as different operating scenarios according to the actual network flow pattern in the system. We note from the results of Figure 5d that the same system security level associated with energy
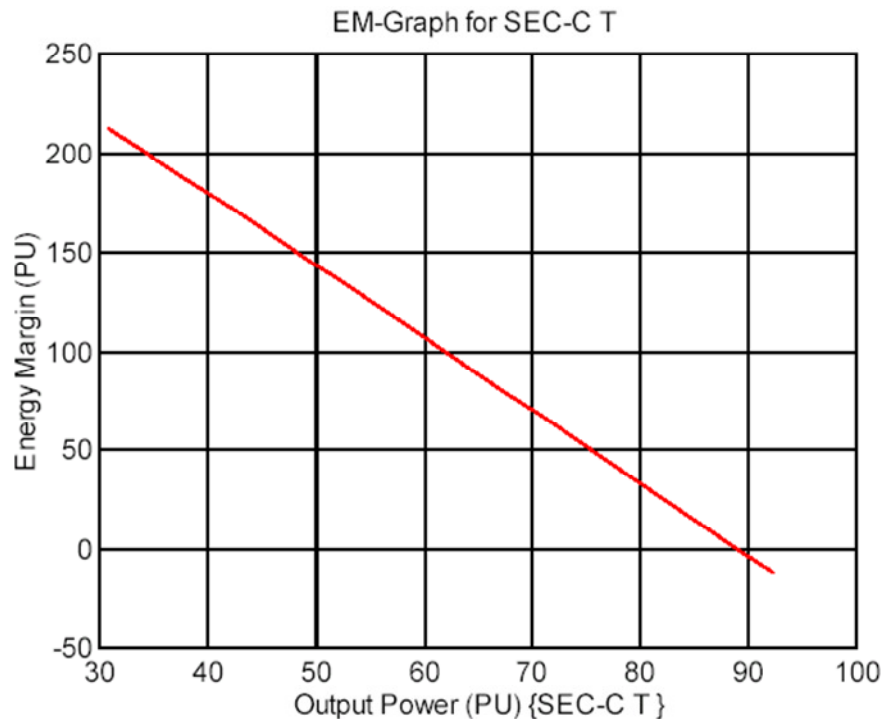
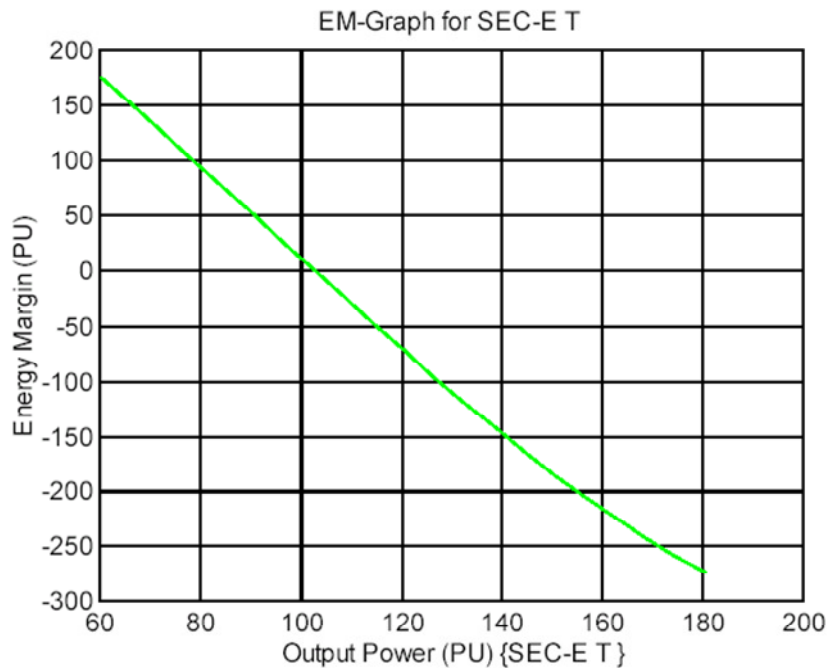**Figure 6a.** Operating security margin versus SEC-C output power.

margin = 2 PU can be obtained through different possible pair-combinations of PP8 and Qassim outputs, including for example {11 PU, 25 PU}, {12.3 PU, 20 PU}, {13.4 PU, 15 PU}, etc.

Operating security in domain of SEC-C and SEC-E powers

In this scenario, the total output powers from both the SEC-Central Region and SEC-Eastern Regions are considered. The associated operating security margin is evaluated in the space spanned by these two output powers. As before, the impacts on system security as a result of variations in the output powers are evaluated using a special simulation module. Figure 6a shows the variation of the operating security margin (energy margin) with SEC-C output power level. It is clear from the results of Figure 6a that the security level decreases as the output power from SEC-C increases. The insecure region (zero energy margin) starts at the SEC-C output level of about 46 PU. The relative system security can be examined using the sensitivity information of Figure 6a. For example, it is noted that increasing the output of SEC-C from 40 PU to 60 PU would cause the energy margin to decrease from 180 PU to about 110 PU. This represents a security deterioration of about 39% for an increase in output power by 50%.

Figure 6b shows the variation of the operating security margin (energy margin) with SEC-E output power level. It is clear from the results of Figure 6b that the security level decreases as the output power from SEC-E increases. The insecure region (zero energy margin) starts at the SEC-E output level of about 6 PU. Again, the sensitivity information of Figure 6b can be used to examine the relative system security. For example, an increase in SEC-E power level by 20 PU from a base operating level of 100 PU would cause the energy margin to decrease from 90 PU to about 10 PU. This represents a security deterioration of about 90% for an increase in output power by only 20%. Comparing this result with that of SEC-C, it is concluded that the relative increase in SEC-E power output has a bigger impact on system security than that of the SEC-C. This finding is confirmed from the results of Figure 6c, which depicts the relationship between the two output powers and the system energy margin.

As in the previous case, the energy margin contours depict possible combined variations of both SEC-C and SEC-E output powers for a given system security level. Figure 6d shows three energy margin contours at 10, 20, and 30 PU values, respectively. Again, it is important to note that in this case, the energy margin contours are evaluated as different operating scenarios according to the actual network flow pattern in the system. We note from the results of Figure 6d that the same system

Figure 6b. Operating security margin versus Qassim output power.

security level associated with energy margin = 10 PU can be obtained through different possible pair-combinations of SEC-C and SEC-E outputs, including for example {45 PU, 400 PU}, {60 PU, 325 PU}, {70 PU, 260 PU}, etc.

Conclusions

This paper has addressed one of the important issues currently of concern to power system operation and management, namely the identification of operating security regions within which the system can operate safely in order to maintain reliable and secure supply of electricity to the consumers. In this regard, the paper has presented a novel framework for identification and representation of operating security regions in power systems as well as evaluation of security levels associated with different operating scenarios. While the concepts and principles presented in the paper are general, the work of this paper is confined to the interpretation of the security boundary in terms of system stability criteria. Nonetheless, the framework presented is applicable quite as well to other criteria that may be considered.

The demonstrative application presented in the paper has revealed several useful observations. Only the binding (active) constraints are used to form the operating security region. In the application presented, the binding constraints represent the system stability limits as well as the minimum load supply requirements. On the other

hand, two operating scenarios were considered in the demonstrative scenario presented in the paper. The evaluated operating security margins associated with the two operating scenarios are 0.92 and 0.07, respectively. The second operating scenario is therefore considered as insecure since any unforeseen deviations in the control parameters around the base operating point could lead to system instability.

The application presented for the Saudi electricity system has revealed several important findings. Several operating scenarios were analyzed in which the total output powers from two power plants or areas were considered. The associated operating security margin was evaluated in the space spanned by these two output powers. A special simulation module was used to evaluate the impacts on system security as a result of variations in the output powers. In the scenario involving both the PP8 power plant and Qassim area, it was noted that the insecure region (zero energy margin) starts at the PP8 output level of about 14 PU. it was also noted that an increase in PP8 power level by 2.5 PU from a base operating level of 10 PU would cause the energy margin to decrease from 24 PU to about 10 PU. This represents a security deterioration of about 58% for an increase in output power by just 25%.

On the other hand, the insecure region (zero energy margin) starts at the Qassim output level of about 11.3 PU. In this case, an increase in Qassim power level by 4 PU from a base operating level of 4 PU would cause the
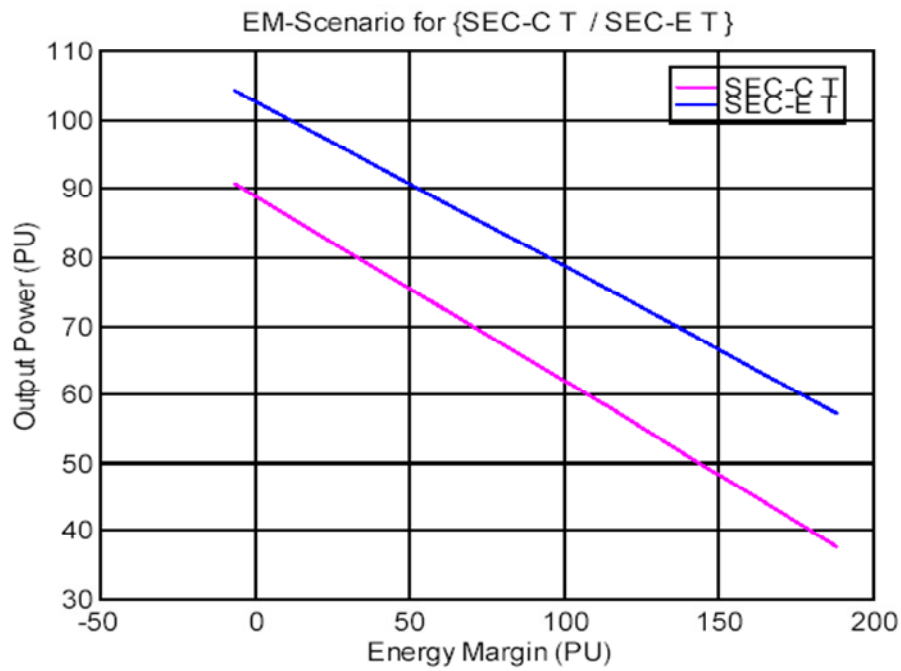
Figure 6c. Relationship between SEC-C and SEC-E output powers and energy margin.
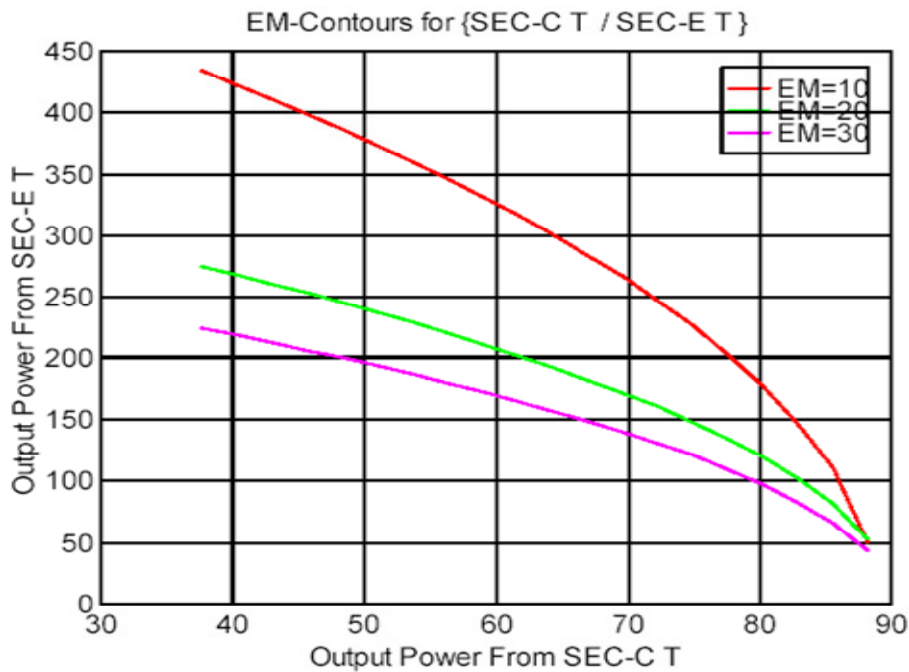

Figure 6d. Energy margin contours in the domain of PP8 and Qassim output powers.

energy margin to decrease from 29 PU to about 13 PU. This represents a security deterioration of about 55% for an increase in output power by 200%. Comparing this result with that of PP8, it is concluded that the relative increase in Qassim power output has a lesser impact on system security than that of the PP8.

For the operating scenario involving the total output powers from both the SEC-Central Region and SEC-Eastern Regions, the simulation results obtained showed that the insecure region (zero energy margin) starts at the SEC-C output level of about 46 PU. It is also noted that increasing the output of SEC-C from 40 PU to 60 PU would cause the energy margin to decrease from 180 PU to about 110 PU. This represents a security deterioration of about 39% for an increase in output power by 50%. On the other hand, the insecure region (zero energy margin) starts at the SEC-E output level of about 6 PU. An increase in SEC-E power level by 20 PU from a base operating level of 100 PU would cause the energy margin to decrease from 90 PU to about 10 PU. This represents a security deterioration of about 90% for an increase in output power by only 20%. Comparing this result with that of SEC-C, it is concluded that the relative increase in SEC-E power output has a bigger impact on system security than that of the SEC-C.

ACKNOWLEDGMENT

REFERENCES

Aghaei J, Shayanfar HA, Amjady N (2009). Joint market clearing in a stochastic framework considering power system security. Appl. Energy, 86: 1675–1682.

Al-Ammar EA, El-Kady MA (2009). Identification of Secure Operating Modes of Power Systems. Final Project Report, Center of Excellence in Information Assurance, King Saud University, August 2009.

Albert MS, Hyde MM (1974). Some Applications of Optimization Techniques to Power systems Problems. IEEE Proc. 62(7).

Allen JW, Bruce FW (1984). Power Generation, Operation and Control. John Wiley & Sons.

Annakkage UD, Jayasekara B (2007). Ensuring power system security against contingencies, Proc. of the II Int. Conf. Industrial Information Syst. ICIIS: 559-564. 8 – 11 August. Sri Lanka.

Athay T, Podmore R, Virmani S (1979). A practical method for direct analysis of Transient energy stability. IEEE Trans. PAS, 98 (March/April 1979): 573-584.

Aven T (2007). A unified framework for risk and vulnerability analysis covering both safety and security. Reliability Eng. Syst. Saf., 92: 745–754.

Benguo Z, Dapeng W, Lei L, Xinsheng N, Hongzhi Z, Yishu Z (2006). Research of Incentive Revelation Mechanism in Power System Optimal Security Control. Int. conf. Power System Proc., 2006(5).

El-Kady MA (1986). (Principal Investigator) Ontario Hydro, Iowa State University. Direct Analysis of Transient Stability for Large Power Systems. EPRI Project No. 2206-1. Final Report No. EL-4980. December 1986.

El-Kady MA, Abu-Elnaga MM, Findlay RD, Bailey CG (1986a). Sparse formulation of the direct method of transient stability for applications on micro computers. Proc. 29th Midwest Symposium on Circuits and Syst. (Lincoln, Nebraska, 1986): 519-522.

El-Kady MA, Al-Ammar EA (2009). Framework for Identification of Power System Operating Security Regions. Proc. of Third Int. Conf. on Network and Syst. Security (NSS 2009), FIAS'09 Workshop.

El-Kady MA, Bell BD, Carvalho VF, Burchett RC, Happ HH, Vierath DR (1986b). Assessment of real-time optimal voltage control, IEEE Trans. Power Syst. PWRS(1): 98-107.

El-Kady MA, Ganton RWD (1989). Fast decoupled transient stability. Canadian Electrical Eng. J., 14(2): 63-66.

El-Kady MA, Tang CK, Carvalho VF, Fouad AA, Vittal V (1986c). Dynamic security assessment utilizing the transient energy function method. IEEE Trans. Power Apparatus Syst. PWRS-1. 284-291.

Popovic DP, Dobrijevic DM, Mijuskovic NA, Vlaisavljevic DJ (2001). An Advanced Methodology for Steady-State Security Assessment of Power Systems. ETEP. 1I (4): 227-233. July/August 2001.

Srivani J, Swarup KS ((2008). Power system static security assessment and evaluation using external system equivalents, Electrical Power Energy Syst., 30: 83–92.

Tomsovic K, Bakken DE, Venkatasubramanian V, Bose A (1993). Designing the Next Generation of Real-Time Control, Communication, and Computations for Large Power Systems. IEEE Proc. 93(5): 965-979.

Zeng Y, Zhang P, Wang M, Jia H, Yu Y, Lee ST (2006). Development of a New Tool for Dynamic Security Assessment Using Dynamic Security Region. Proc. of the 2006 Int. Conf. Power Syst. Technol., p. 5.